

AD-A122 789 THE PHENOMENA OF TARGETS IRRADIATED BY AN INTENSE CO2 LASER(U) FOREIGN TECHNOLOGY DIV WRIGHT-PATTERSON AFB OH 1/1
5 XIA ET AL. 09 NOV 82 FTD-ID(R5)T-0952-82

AD-A122 789 THE PHENOMENA OF TARGETS IRRADIATED BY AN INTENSE CO2 LASER(U) FOREIGN TECHNOLOGY DIV WRIGHT-PATTERSON AFB OH 1/1
5 XIA ET AL. 09 NOV 82 FTD-ID(R5)T-0952-82

AD-A122 789 THE PHENOMENA OF TARGETS IRRADIATED BY AN INTENSE CO2 LASER(U) FOREIGN TECHNOLOGY DIV WRIGHT-PATTERSON AFB OH 1/1
5 XIA ET AL. 09 NOV 82 FTD-ID(R5)T-0952-82

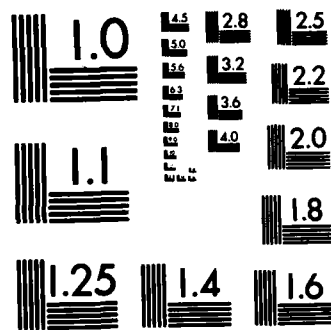
UNCLASSIFIED F/G 20/5 NL

UNCLASSIFIED F/G 20/5 NL

UNCLASSIFIED F/G 20/5 NL

6. 11. 01

4



MICROCOPY RESOLUTION TEST CHART
NATIONAL BUREAU OF STANDARDS-1963-A

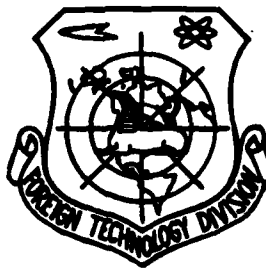
FOREIGN TECHNOLOGY DIVISION



THE PHENOMENA OF TARGETS IRRADIATED BY
AN INTENSE CO₂ LASER

by

Xia Shengjie, Wang Chunkui, et al



DTIC
ELECT
DEC 20 1982

Approved for public release;
distribution unlimited.

82 12 29 013

AD A122789

DTIC FILE COPY

EDITED TRANSLATION

FTD-ID(RS)T-0952-82

9 November 1982

MICROFICHE NR: FTD-82-C-001451

THE PHENOMENA OF TARGETS IRRADIATED BY AN INTENSE
CO₂ LASER

By: Xia Shengjie, Wang Chunkui, et al

English pages: 16

Source: Wuli Xuebao, Vol. 31, Nr. 3, March 1982,
pp. 397-403

Country of origin: China

Translated by: LEO KANNER ASSOCIATES
F33657-81-D-0264

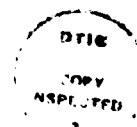
Requester: FTD/TQTD

Approved for public release; distribution unlimited.

| | |
|--------------------|-------------------------------------|
| Version For | |
| GRACI | <input checked="" type="checkbox"/> |
| Other | <input type="checkbox"/> |
| Unpublished | <input type="checkbox"/> |
| Availability Codes | |
| Dist | Special |
| A | |

THIS TRANSLATION IS A RENDITION OF THE ORIGINAL FOREIGN TEXT WITHOUT ANY ANALYTICAL OR EDITORIAL COMMENT. STATEMENTS OR THEORIES ADVOCATED OR IMPLIED ARE THOSE OF THE SOURCE AND DO NOT NECESSARILY REFLECT THE POSITION OR OPINION OF THE FOREIGN TECHNOLOGY DIVISION.

PREPARED BY:
TRANSLATION DIVISION
FOREIGN TECHNOLOGY DIVISION
WP-AFB, OHIO.



GRAPHICS DISCLAIMER

All figures, graphics, tables, equations, etc. merged into this translation were extracted from the best quality copy available.

The Phenomena of Targets Irradiated by an Intense CO₂ Laser

by Xia Shengjie, Wang Chunkui, Fu Yushou, Wu Baogen, Fang Huiying, Zhou Guangdi

(Institute of Mechanics, Academia Sinica)

Abstract

Using the continuous and pulsed CO₂ laser as the main light source,, we first studied the phenomena produced in the area in front of the target for the effects of the intense laser on target material. Diagnosis was done by high-speed interferography and we distinguished the forming-time of the crater and the processes of torsion of the direction of the vapor plume produced by the continuous laser. We have also observed the development of the plasma, the air breakdown and unluminous phenomena such as the vapor plume, shock wave etc. produced by the pulsed laser. The high-speed interferography device with pulsed He-Ne laser was used.

Preface

There have been many studies carried out both domestically and abroad on the interaction of lasers and materials. There has been a conference every two years on laser interaction and plasma and one symposium each year on laser damage to optical materials; all of these conferences publish collections of papers [1, 2]. These works center on the actions of lasers and target spheres in order to study man-made fusion; the intense laser on optical materials, especially the damage of high powered laser window, laser treatment and processing etc. The power density range of the laser used is very broad and thus the study of objects is multifold and active. This paper is only concerned with the interaction of intense lasers with relatively low target power density range and the solid target materials. At present, high-speed photography is commonly

used as the diagnostic technique for experimental research on these problems. Among these, most are concerned with researching luminous phenomena [3-5]. However, for the study of unluminous phenomena, aside from seeking aid from high-speed photography, it is also necessary to employ optical display techniques. At present, high-speed interferography, the high-speed shadow technique [7] and schieren technique are used in these studies. They are used to diagnose the phenomena produced in the area in front of the target when there is laser-target material action; for example, the study of the formation and development etc. [6] of the laser sustaining detonation wave (LSD). The pulsed He-Ne laser separate amplitude high-speed interferography and shadow technique [7] developed by us are used to diagnose the phenomena in the area in front of the target when there is laser-target material interaction. When researching the continuous and pulsed CO₂ laser irradiation of metallic and non-metallic target materials, many luminous phenomena are recorded. Several tens of interferographs on the interaction process can be obtained from each experiment.

The Action of the Continuous Output Laser and the Target Material

A focus lens with a focal length of 135 millimeters is used in research on the interaction of the 70 watt continuous output power CO₂ laser and the target material [8]. A light beam spot of about 0.5 millimeter in diameter is focused on the target and a power density of 3×10^4 watts/centimeter² is obtained. The target material has both melting and a large amount of vaporization on this power density level. The vapor plume jet speed produced by the laser is relatively low and is related to characteristics of the target material. We used two types of typical material: ceramic and organic glass. The instant we use high-speed interferography to diagnose the laser beam action

on the target we immediately obtain the process of dynamic balance.

We can see from high-speed interferographs 1-4 that the vapor plume initially produced on the target material assumes a columnar structure.

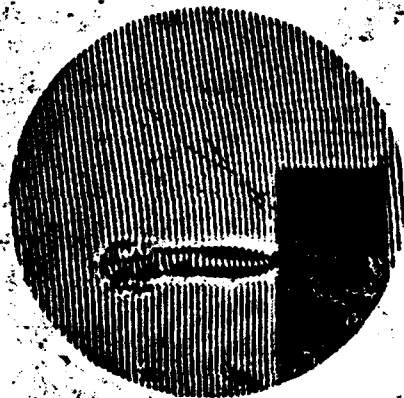


Fig. 1 Columnar Structure of the Organic Glass Vapor Plume



Fig. 2 Steady Spray of the Organic Glass Vapor Plume

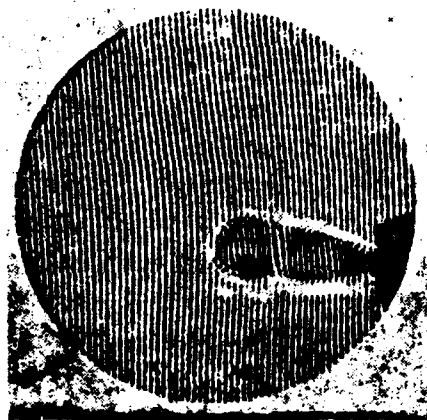


Fig. 3 Columnar Structure of the Ceramic Vapor Plume



Fig. 4 Vapor of the Ceramic Vapor Plume and the Burst Open Vapor Mass

See fig. 5 for the vapor plume spray contour of the two types of materials.

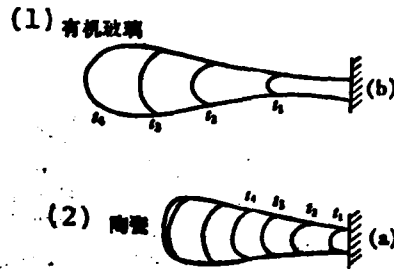


Fig. 5 The Forms of the Vapor Plumes Change With the Time

Key: 1. Organic glass
2. Ceramic

The initial spray speed of the organic glass vapor plume is 3.6×10^2 centimeters/second. Although the energy of the laser beam is steady from the initial incidence to the final stage, yet the growth speed of the vapor plume's leading edge is changing as is shown by the curves in fig. 6.

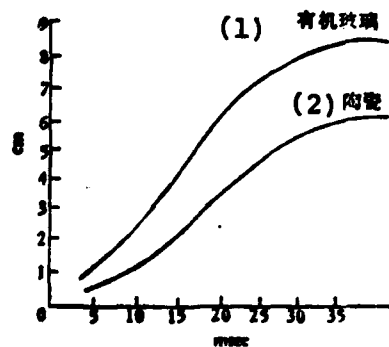


Fig. 6 The Relational Curves of the Vapor Plume's Leading Edge Shift and the Time

The vertical coordinate is cm and the horizontal coordinate is msec

Key : 1. Organic glass
2. Ceramic

The vapor plume facing the radiation with wavelengths of 10.6 and 0.6328 micrometers is basically transparent and during the spraying process it cannot further absorb energy. The interference fringes within the plume can be seen in figures 1-4. The original temperature and density in the vapor plume, which is larger than that of the surrounding gas, gradually decreases during the spraying process and when it sustains air resistance, the vapor plume will continually spread open. This will cause the spraying process to reach a state of dynamic equilibrium. In the end, the speed along the normal direction of the target decreases to zero and forms a continuous and steady spraying process as shown in fig. 2.

As regards the ceramic material during the initial period of laser action, it is within about 5 milliseconds, its phenomena are similar to those of organic glass and the vapor plume is a columnar structure as well as transparent as shown in fig. 3. However, the initial spraying speed of the vapor plume is lower than that of organic glass, about 1.9×10^2 centimeters/second. During a later period, the scouring effect causes this type of heat insulated powder sintering body to form independent vapor masses when the globular powder is vaporized by the heat. There are also condensed particles which are sprayed out with the vapor plume. Yet these particles are not transparent and during the spraying out process they will continually absorb a portion of the optical radiation. Because the sprayed out vapor mass is located in an environment with relatively low pressure and temperature, it bursts open in the vapor plume. We can see the path of the bursting particles clearly in fig. 4. The centers of their bursting are not necessarily on the target but rather in the area in front of the target.

It can be seen from the negatives of a series of high-speed interferographs that the spray of the ceramic material's vapor plume is not steady like that of the organic glass but has non-periodic pulsation. Steady laser energy cannot continually radiate on the target material. The sprayed particles and vapor create interference for the incidence of light and a good deal of energy is consumed.

The vapor plume produced by the laser irradiation of the target material always begins to spray outwards of the vertical target. To distinguish these phenomena, the target and incidence laser beam form a 45° angle. The laser beam operates in the instant of the target material and the vaporized substance is vertical to the 45° angle formed by the target and laser incidence direction as shown in fig. 7(a). However, the target lengthens with time and after forming craters and paths, the vapor plume very quickly turns to spray in the opposite incident light direction. We can see the process of torsion of this type of spraying direction from fig. 7. The beginning torsion of the organic glass is about 20 milliseconds and the torsion ends at 33 milliseconds. This is also the time for forming craters.

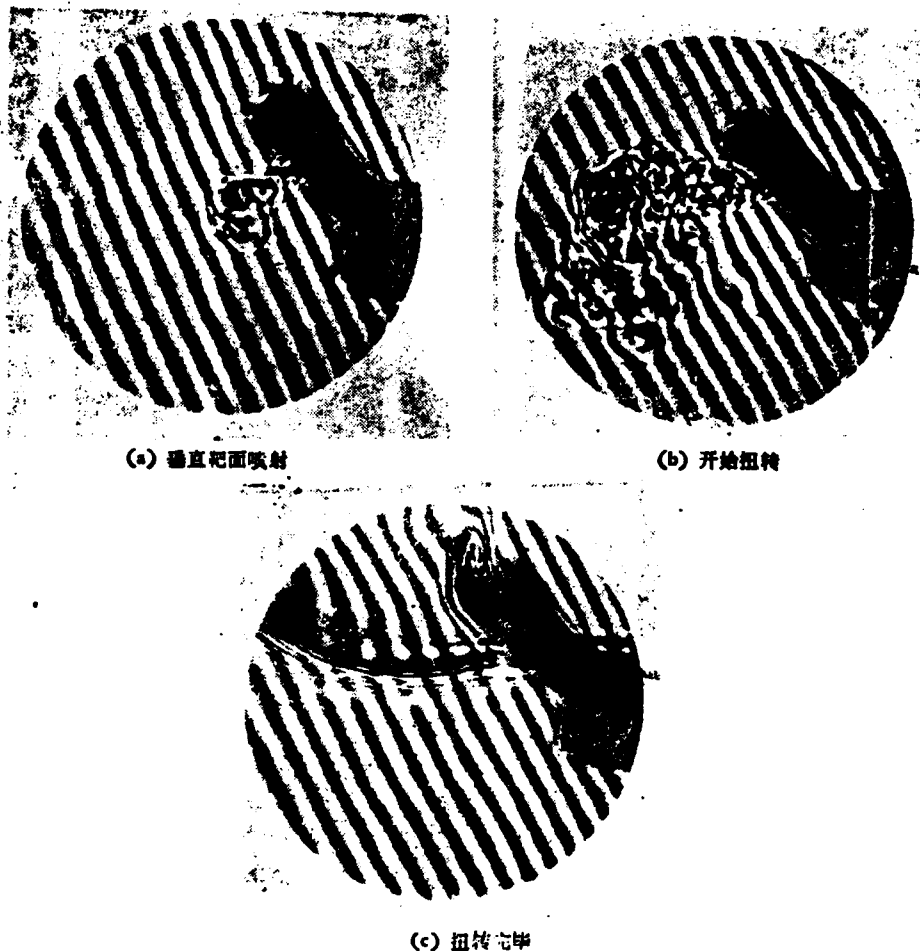


Fig. 7 Torsion Process of the Vapor Plume

- (a) Vertical target spray
- (b) Beginning torsion
- (c) Torsion completed

When a laser with a continuous output of 30,000 watts focuses a 1,000 millimeter range focusing range mirror on a stainless steel target, we can observe a great deal of high temperature metallic melted drop spattering which forms dazzling sparks. This does not exist in non-metallic ablation as shown in fig. 8. The melted drops in the light beam angle must still continuously absorb the optical radiation and therefore it is often

necessary to use high pressure gas to blow and scatter the melted drops. Thus, even more light can radiate on the target.

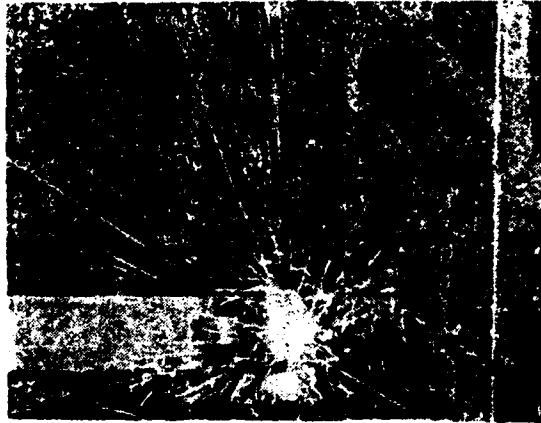


Fig. 8 Circumstances of an Intense Laser Irradiating a Metallic Target

The Action of the Pulsed CO_2 Laser and Target Material

A TEA CO_2 pulsed laser beam which uses 10 joule energy and has a pulse width of 1 microsecond focuses a lens with a focusing length of 100 millimeters on a target. When the power density reaches to an energy level of about 10^7 watts/centimeter², the target material is dominated by vaporization [10]. The instant the laser acts on the target material there is produced high temperature and vaporized target material. The vaporized substance instantly expands outward along the vertical of the target, compresses the air in front of the target and forms a circular air shock wave and outward propagation using the place where the light beam comes in contact with the target point as the center. After the laser beam is finished, the top part of the vaporized substance rapidly diffuses into a mushroom shape. Its leading edge speed quickly decreases. The phenomena of the circular shock wave and vertical target spray

as well as the final formation of the mushroom shaped vapor plume can be seen from figures 9 and 10.

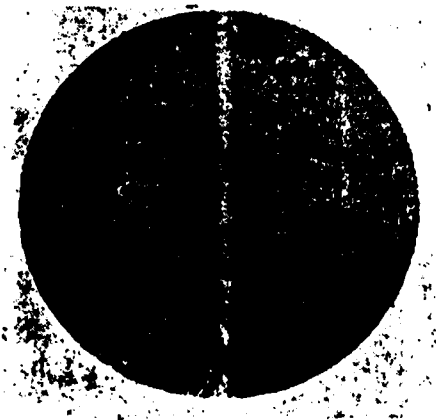


Fig. 9 Circular Shock Wave



Fig. 10 Mushroom Shaped Vapor Plume

The shock wave propagates outward with supersonic speed. The initial Mach number is about 1.84 and continues until the shock wave disappears. This process does not have intense light or noise. The greater part of the light beam energy can couple with the target material. When the target crater is relatively

deep, the ablation area is equal to the measurement of the spot and there is a noticeable perforated effect.

The Pulsed CO_2 Laser Exceeds the Breakdown Threshold

When the pulsed CO_2 laser's power density is increased to the 10^9 watts/centimeter² level, the power density far exceeds the breakdown threshold. When the laser is focused on a target in an atmospheric environment, this causes air breakdown in front of the target and also produces high temperature plasma. Moreover, there is accompanying intense light and noise. The plasma cloud along the direction of the light beam is a major axis which forms an ellipsoidal air shock wave with the plasma cloud as the center which propagates outward. The plasma cloud's center is in front of the target and the ellipsoidal shock wave hits the target and forms a reflected wave. We can see from the tests shown in figures 11 and 12 that the target forms a 45° angle with the incident laser.



Fig. 11 Ellipsoidal Plasma Cloud



Fig. 12 Ellipsoidal Shock Wave, Reflected Wave and Mach Reflection

Fig. 13 draws the original ellipsoidal shock waves of each time period and the reflected waves on an inclined target.

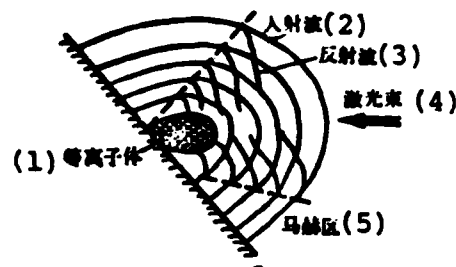


Fig. 13 The Incident Reflection of the Ellipsoidal Shock Waves When Producing Detonation Waves

- Key: 1. Plasma
2. Incident wave
3. Reflected wave
4. Laser beam
5. Mach area

When the reflected waves are transmitted in a dielectric which

is passed through and heated by the original waves, their absolute speed is greater than the original waves. Thus, they overtake the original waves and form Mach number reflection [12] as shown in the lower portion of fig. 12. This has the same results as the reflection of the point source detonation shock waves on a wall surface [9] as shown in fig. 14.

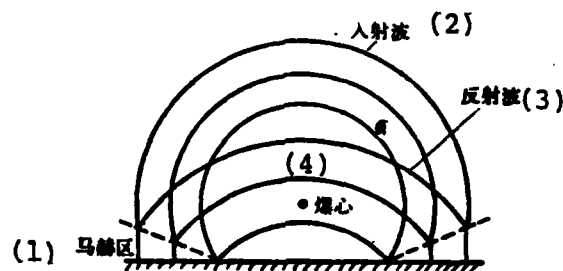


Fig. 14 Incident Reflection of Atomic Detonation Circular Shock Waves

- Key: 1. Mach area
 2. Incident wave
 3. Reflected wave
 4. Detonation center

32 microseconds after the laser breaks down the air and the reflected wave passes a residual area with high temperature and high density boundary, the waveform appears hysteretic and non-continuous as shown in fig. 12. This is the result of the interaction of the plasma and the air shock wave. If the distance between the plasma's center and the target enlarges, then when the reflected wave reaches this area there will not be hysteresis and non-continuity in front of the wave.

From the direct determination of the luminous plasma in a

high-speed photograph, about 16 microseconds after the pulsed laser with the above mentioned power density is finished, the expansion along the edge of the plasma cloud reaches a maximum value of about 6 millimeters. The plasma's high temperature radiation acts on the target material to produce an ablation area much larger than the measurement of the laser beam spot. After the plasma which develops in the direction of the laser beam disappears we see a columnar vaporized plume which forms a 45° angle with the light beam and which is vertical to the target. Its bottom part widens as shown in fig. 11. This is in obvious contrast with figures 8 and 9.

The Influence of the Breakdown Threshold on Material Damage

In comparing test figures 9, 10 and 11, when the laser power density is below the air breakdown threshold, a circular shock wave is produced, the vaporized substance is vertical to the target spraying and the bottom part is very small. Different target materials have different ablation depths. When the power density exceeds the breakdown threshold, the air is broken down and forms an ellipsoidal wave. At this time, the quality of the target material moves to a position of secondary importance. The effects of the interaction of different target materials is approximately the same as the laser. Determined from the final crater on the target, after producing plasma, the ablation area of the target area is one quantity level greater than when there is no breakdown. The shape is not uniform and the crater is relatively shallow. The laser energy does not completely and directly act on the target but is the result of the high temperature plasma cloud's reirradiation of the target. Therefore, when the laser energy is greater than or smaller than the air breakdown threshold, different damage effects are produced on the target material. This is significant for the study of the interaction of lasers and target material in an atmospheric

environment, especially for laser perforation.

The Spray Direction and Torsion of Continuous and Pulsed Laser Vapor Plume

As regards the diagnostic photographs of continuous and pulsed laser irradiation of target material with a 45° angle of inclination, strong lasers which exceed the air breakdown threshold cause plasma and ellipsoidal shock waves to form in front of the target along the light beam direction. About several tens of microseconds after the pulsation stops and the plasma disappears, only a columnar vapor plume exists at a 45° angle with the light beam and vertical to the target. As a result, the plasma and vapor plume form a 45° angle under these test conditions. The elliptical shock waves continue to propagate and the ellipticity increases.

There is no noticeable plasma and noise for lasers below the breakdown threshold and there is only vapor plume and circular shock waves vertical to the target.

When compared with the above mentioned circumstances, because of the formation of ablation passages in the continuous laser action process, the spray direction of the vapor plume has a torsion process. The stronger the light beam the faster the torsion. It is about several tens of milliseconds for non-metallic materials.

Conclusion

The above mentioned tests showed several points: the spraying of vapor plume caused by the continuous laser is always vertical to the target surface and assumes a columnar shape in the initial stages of various types of target materials. The

direction changes only because of the formation of craters. When the laser continually irradiates the crater deepens which is unrelated to the target's position angle; we must control the high and low of the threshold for the pulsed laser and target material action in order to have different effects. When perforation is needed, the power density should not exceed the breakdown threshold. In this way, deep holes with standard measurements can be attained.

Further, the developed pulsed He-Ne laser separate amplitude high speed interferographic device can record luminosity, especially the developmental process of un luminous phenomena. It provides a great deal of two dimensional information for phenomena produced in transparent mediums; for example, diagnosis of phenomena in front of the target when there is laser-target action. It is an excellent diagnostic method.

References

- [1] G.V. Sklizkov, Laser interaction and related plasma phenomena, (1971).
- [2] Glass and Guenther, Laser induced damage in optical materials.
- [3] W.E. Maher, R.B. Hall, R.R. Johnson, J. Appl. Phys., 45(1974), 3675.
- [4] R.L. Stegman et al., J. Appl. Phys. 44(1973), 2138.
- [5] S.A. Metz, J. Appl. Phys., 46 (1975), 1634.
- [6] R.B. Hall, W.E. Maher & P.S.P. Wei, AD-766766; (1973).
- [7] Xia Shengjie et al., International conference on laser 1980 digest, p. 172.
- [8] Zhou Guangdi, Xia Shengjie et al., Lasers, 5 (1978).
- [9] Lin San et al., tr., Collection of Essays on Atomic Weapons, National Defense Publications.
- [10] G. Varsi, author, Changsha Engineering College, tr., Laser Technology 5.
- [11] John F. Ready, Effects of high-power laser radiation, (1971).
- [12] L.L. Glass, Shock waves and man, (1974).

2-8

DT